Appl Phys B (2011) 104:969–974
DOI 10.1007/s00340-011-4630-0

Applied Physics B
Lasers and Optics

Oxygen isotope separation utilizing two-frequency infrared multiphoton dissociation of 2,3-dihydropyran

M. Hashimoto · H. Ohba · A. Yokoyama

Received: 10 December 2010 / Revised version: 12 May 2011 / Published online: 8 July 2011
© Springer-Verlag 2011

Abstract Oxygen isotope separation has been examined by utilizing the two-frequency infrared multiphoton dissociation (IRMPD) of 2,3-dihydropyran (DHP). The two-frequency IRMPD reduces the required laser fluences to those lower than the damage threshold of optical windows. For example, dissociation probability of DHP containing ^{18}O (D(^{18}O)) and enrichment factor (S) were obtained to be 1.6×10^{-3}/pulse and 316, respectively, by the simultaneous irradiation with 1052.2 cm^{-1} photons at 0.45 J/cm^2 and 1031.5 cm^{-1} photons at 1.06 J/cm^2. These are comparable with D(^{18}O) $= 2.2 \times 10^{-3}$/pulse and $S = 391$ obtained by the single-frequency irradiation of 1033.5 cm^{-1} photons at 2.2 J/cm^2. Therefore, the production rate of an ^{18}O enriched dissociation product has been increased to four times or more, compared with the single-frequency IRMPD, and this two-frequency method would promise a practical large scale separation.

1 Introduction

Natural oxygen consists of three stable isotopes, ^{16}O, ^{17}O and ^{18}O, whose natural abundances are 99.759% (^{16}O), 0.037% (^{17}O) and 0.204% (^{18}O). The ^{18}O isotope is widely used as an essential radio-pharmaceutical material for the production of ^{18}F-fluorodeoxy glucose which is used for the positron emission tomography diagnoses of cancers. Isotope enrichment of oxygen has already been performed by various methods, such as membrane distillation [1], cryogenic distillation [2–4], chemical exchange [5], electrophoresis [6], liquid chromatography [7, 8], electrolyte cells [9], plasma chemical reactions [10, 11], and IRMPD [12–14]. The enrichment of ^{18}O has been done commercially by the distillation of O_2, NO, and H_2O. However, the enrichment factor (S) of ^{18}O, which is defined as the ratio of the [^{18}O]/[^{16}O] in the gas phase to that in the liquid phase during the distillation, is very low. For example, the enrichment factor is only 1.006 for the distillation of O_2 at 90 K [2–4]. Consequently, the distillation plant has to become a huge system with many distillation towers needed to get many theoretical plates; by this plate we mean a hypothetical stage in which the equilibrium between liquid and vapor phases is established. Similarly, the enrichment factors for other methods except for IRMPD are also small; 1.034 for the chemical exchange, 1.017 for the liquid chromatography, 1.03 for the electrolyte cells, and ∼2 for the plasma chemical reaction.

On the other hand, the IRMPD method shows intrinsically large enrichment factor. Especially, the IRMPD of diisopropyl ether, $(C_3H_7)_2O$, showed a large enrichment factor of 350 [13]. Although the enrichment factor was large enough, the dissociation probability of $(C_3H_7)_2{}^{18}O$ was small (less than 3×10^{-4}/pulse). Furthermore, the IRMPD of $(C_3H_7)_2O$ produces radicals as primary products through the C–O bond rapture, and then the secondary reactions occur immediately. Therefore, the selectively separated oxygen isotope distributes in several products, and the isotope scrambling may also occur. So, it is important to find other suitable reactants for IRMPD which show

M. Hashimoto (✉) · A. Yokoyama
Quantum Beam Science Directorate, Kansai Photon Science Institute, Japan Atomic Energy Agency, Kizugawa, Kyoto 619-0215, Japan
e-mail: hashimoto.masashi22@jaea.go.jp
Fax: +81-774-713338

A. Yokoyama
e-mail: yokoyama.atsushi@jaea.go.jp

H. Ohba
Quantum Beam Science Directorate, Tokai Research and Development Center, Japan Atomic Energy Agency, Tokai, Ibaraki 319-1195, Japan
e-mail: ohba.hironori@jaea.go.jp

large dissociation probability, large isotope selectivity, and no secondary reaction. We found that 2,3-dihydropyran (C_5H_8O; DHP) was a suitable candidate fulfilling these requirement. The DHP dissociates concertedly into two stable molecules, 2-propenal (C_3H_4O) and ethylene (C_2H_4), through the retro Diels–Alder reaction [15]. We succeeded in the enrichment of ^{18}O with the large dissociation probability (2.2×10^{-3}/pulse) and high enrichment factor (391) by the IRMPD of DHP at the laser fluence of 2.2 J/cm^2 [16]. However, because the laser fluence was higher than the damage threshold of a reaction cell window the laser beam had to be focused into the cell by a lens to prevent damage to the cell windows. In this irradiation geometry, the reaction zone is limited around the focus. This is unfavorable to a large-scale isotope separation. Therefore, it is essentially important to increase the isotope production rate at the laser fluence below the damage threshold of the windows. For the reduction of the required laser fluence, we have introduced the two-frequency IRMPD scheme in the silicon isotope separation and succeeded in reducing the laser fluence while keeping the dissociation probability [17, 18]. In this work, we examine the effect of the two-frequency irradiation scheme on the oxygen isotope separation by the IRMPD of DHP.

2 Experiment and analysis

2,3-dihidropyran and 2-propenal, the stated purities being more than 98% and 95%, respectively, were purchased from Tokyo Kasei Co. LTD and used without further purification without degassing at 77 K. The experimental apparatus is similar to that used previously [17]. Briefly, a Lumonics TEA-841 CO_2 laser and an Ushio UGL-TEA-3C CO_2 laser were used as the excitation and dissociation photon sources, respectively. The reaction cell was made of stainless steel with a NaCl window at both ends. The total volume (V_0) of the cell was 44.5 cm^3. DHP in the cell was irradiated at the 1–3 Hz by two CO_2 laser lights. The laser beams were counter-propagating in the cell after having been collimated through an iris with the open area of 0.44–0.52 cm^2. The volume (V_i) of the irradiated region was 4.4–5.2 cm^3. The pulse energy of each laser was controlled by inserting a ZnSe beam splitter or CaF_2 plates into the laser beam line, and monitored with a pyroelectric joulemeter (Gentec ED-500). The pulse delay between two laser beams was set within 50 ns using a pulse delay generator (Stanford Research DG-535).

Concentrations and isotopic compositions of 2-propenal in the cell before and after irradiation were obtained from GC/MS spectra taken by a GC/MS instrument (Shimadzu GCMS-QP2010) with a 60 m DB-1 widebore capillary column (J&W Scientific).

The isotopic fractions of oxygen in C_3H_4O were determined from the signal intensities at $m/e = 55(^{12}C_3H_3{}^{16}O^+)$, $56(^{12}C_3H_4{}^{16}O^+)$, $57(^{12}C_2^{13}CH_4{}^{16}O^+, {}^{12}C_3H_3{}^{18}O^+)$, and $58(^{12}C_2^{13}C_2H_4{}^{16}O^+, {}^{12}C_3H_4{}^{18}O^+)$ as described in [16]. The dissociation probabilities of $C_3H_4{}^{18}O$ and $C_3H_4{}^{16}O$, which are defined as the dissociation fraction of the respective isotopic molecules in the overlap region between the lasers in the cell after the one shot irradiation and denoted respectively as D(^{18}O) and D(^{16}O), are calculated from the ^{18}O isotopic fraction [f(^{18}O)] in C_3H_4O produced after the irradiation of n shots as follows [16]:

$$\mathrm{D}(^{18}\mathrm{O}) = -\frac{V_0}{V_i n}\ln\left\{1 - \frac{f(^{18}\mathrm{O})}{0.00204(1 + [C_5H_8O]/[C_3H_4O])}\right\}, \tag{1a}$$

$$\mathrm{D}(^{16}\mathrm{O}) = -\frac{V_0}{V_i n}\ln\left\{1 - \frac{1 - f(^{18}\mathrm{O})}{0.99796(1 + [C_5H_8O]/[C_3H_4O])}\right\}, \tag{1b}$$

where the ratio $[C_5H_8O]/[C_3H_4O]$ can be determined from the signal intensity ratio of $C_5H_8O^+$ to $C_3H_4O^+$ with a correction factor determined using standard mixtures of C_5H_8O and C_3H_4O.

3 Results and discussion

3.1 Frequency dependence of dissociation probability

In general, the vibrational frequency of a molecule in a vibrational excited state shifts to a lower energy side, as the number of absorbed photons increases, as a result of vibrational anharmonicity. Therefore, isotope selective two-frequency IRMPD consists of the selective excitation of $C_5H_8{}^{18}O$ to quasi-continuum states by the excitation laser at low fluence, and the further excitation and dissociation of the molecules in the quasi-continuum states by the dissociation laser at the nearly resonant lower frequency and relatively high fluence.

Figure 1 shows the excitation laser frequency dependence of D(^{18}O), D(^{16}O), and the enrichment factor of ^{18}O [S = D(^{18}O)/D(^{16}O)], together with the IR spectrum of DHP. The predicted absorption spectrum of $C_5H_8{}^{18}O$, which is just shifted that for natural DHP to lower wave number side by the calculated isotope shift (15.1 cm^{-1}), is also shown as broken line. The isotope shift was calculated by an ab initio Molecular Orbital (MO) theory at B3LYP/6-31G(d,p) level using a Gaussian 03 package [19]. The dissociation laser frequency is fixed at 1031.5 cm^{-1}. The fluences of excitation and dissociation lasers are 0.45 and 1.06 J/cm^2, respectively. Although D(^{18}O) and D(^{16}O) tend to increase with increasing the excitation laser frequency because of the laser frequency approaching the absorption peak, those at 1055.7 cm^{-1} show minimum. On the other hand, the enrichment factor is almost constant within the experimental

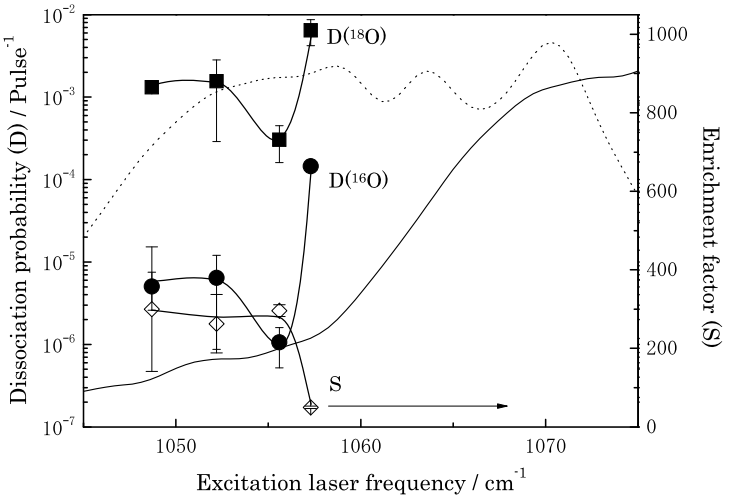

Fig. 1 Excitation laser frequency dependence of dissociation probabilities of DHP (*D*) and isotope enrichment factor (*S*). Sample pressure is fixed at 267 Pa. Excitation laser fluence is 0.45 J/cm^2. Dissociation laser frequency and fluence are fixed at 1031.5 cm^{-1} and 1.06 J/cm^2, respectively. The plots indicate (■) $C_5H_8{}^{18}O$, (●) $C_5H_8{}^{16}O$, and (◇) enrichment factor of ^{18}O, respectively. The *solid curve* indicates the absorption spectrum for the natural DHP, and the broken curve indicates one for $C_5H_8{}^{18}O$ predicted by the calculated isotope shift

error except for one at 1057.3 cm^{-1}. The small increase of the dissociation probabilities around the frequencies lower than 1055.7 cm^{-1} may be due to small absorption attributed to the C–C stretching mode. Since the isotope shift of this vibrational mode is calculated to be 2 cm^{-1} by the ab initio MO theory, it is reasonable that both D(^{18}O) and D(^{16}O) show similar increase around this frequency region. This enhancement of the dissociation probability resulting form a small absorption mode was also observed in the IRMPD of Si_2F_6 [17].

Figure 2 shows the dissociation laser frequency dependence of D(^{18}O) and D(^{16}O). The excitation laser frequency is fixed at 1055.6 cm^{-1} or 1052.2 cm^{-1}. The dissociation probabilities at the excitation laser frequency of 1055.6 cm^{-1} decrease with decreasing dissociation laser frequency, while those at 1052.2 cm^{-1} are nearly constant at low frequencies. The decrease of D(^{18}O) and D(^{16}O) with decreasing the dissociation laser frequency indicates that the absorption peak of the molecules excited in the quasi-continuum states is at the frequency equal to or higher than 1041.3 cm^{-1}. The different behavior between the cases of the excitation at 1052.2 and 1055.7 cm^{-1} may be due to the difference in the average excitation energy after the irradiation of the excitation laser. The average excitation energy is expected to be higher at 1052.2 cm^{-1} than at 1055.7 cm^{-1}, because the dissociation probability at 1052.2 cm^{-1} is about 6 times as high as that at 1055.7 cm^{-1} as shown in Fig. 1. The absorption spectrum of the vibrationally hot molecules is red-shifted and broadens, which is due to the vibrational anharmonicity [20]. Therefore, the absorption spectrum of the molecules in the higher vibrational states, which correspond to the case that the excitation laser frequency is 1052.2 cm^{-1}, is expected to be shifted to a lower frequency and broader. In Fig. 3, the dependence of the enrichment factor of ^{18}O on the dissociation laser frequency is shown. The factor obtained at the excitation laser frequency of 1055.7 cm^{-1} increases monotonically with the

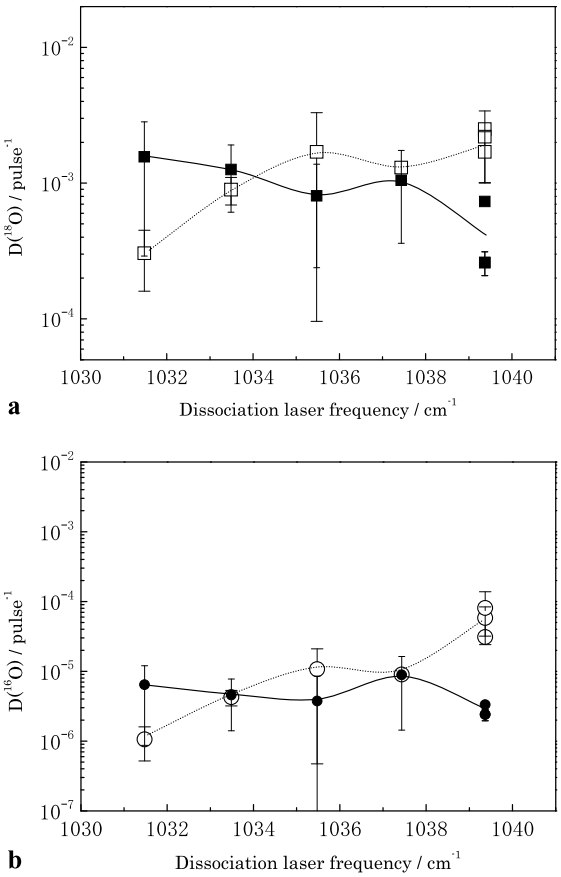

Fig. 2 Dependence of the dissociation probability of (**a**) $C_5H_8{}^{18}O$ and (**b**) $C_5H_8{}^{16}O$ on the dissociation laser frequency. Sample pressure is fixed at 267 Pa. Excitation and dissociation laser fluence are fixed at 0.45 and 1.06 J/cm^2, respectively. The *filled symbols* (■ and ●) indicate the results at the excitation laser frequency of 1052.2 cm^{-1}, and *open symbols* (□ and ○) indicate the results at 1055.7 cm^{-1}

decrease in the dissociation laser frequency, while the factor at the excitation laser frequency of 1052.2 cm^{-1} is nearly constant below 1035 cm^{-1}. Although the enrichment fac-

tors obtained at the excitation laser frequencies of 1052.2 and 1057.7 cm^{-1} are nearly equal at the dissociation laser frequency of 1031.5 cm^{-1}, D(^{18}O) is higher at 1052.2 than at 1057.7 cm^{-1} as shown in Fig. 2(a). Therefore, the pressure and fluence dependences of D(^{18}O), D(^{16}O), and S described below were taken at the excitation and dissociation laser frequencies of 1052.2 cm^{-1} and 1031.5 cm^{-1}, respectively.

3.2 Fluence and pressure dependence of dissociation probability

Figure 4(a) shows the dependence of the dissociation probability and enrichment factors on the excitation laser fluence. The dissociation laser fluence is fixed at 1.13 J/cm^2. Similarly, the dependence on dissociation laser fluence at the fixed excitation laser fluence of 0.45 J/cm^2 is shown in Fig. 4(b). The dependence of D on the fluence Φ is well fitted to the following equation:

$$D = A\Phi^m. \tag{2}$$

The least squares fittings of the data in Fig. 4(a) give $m = 4.6 \pm 2.2$ and 3.5 ± 1.5 for D(^{16}O) and D(^{18}O), respectively. Similarly, the fittings of the data in Fig. 4(b) give $m = 12.8 \pm 3.6$ and 9.9 ± 3.2 for D(^{16}O) and D(^{18}O), respectively. Since D(^{16}O) increases more rapidly than D(^{18}O) with increasing the excitation or dissociation laser fluence, S decreases with increasing fluence. To increase the dissociation laser fluence is advantageous in enhancing the dissociation probabilities, because the value of m is larger for the dissociation laser than for the excitation laser. It should be noted that the decrease fractions of the enrichment factor for both cases are almost the same within the experimental error.

The sample pressure dependence of the dissociation probabilities is shown in Fig. 5. The excitation and dissociation laser fluence are fixed at 0.45 and 1.06 J/cm^2, respectively. Both of D(^{18}O) and D(^{16}O) decrease with increasing pressure as a result of collisional de-excitation. The enrichment factor increases with increasing pressure below 267 Pa and becomes nearly constant at 267 Pa or more. Therefore, the pressure should be below 267 Pa to establish both of high enrichment factor and high dissociation probability of $C_5H_8{}^{18}O$.

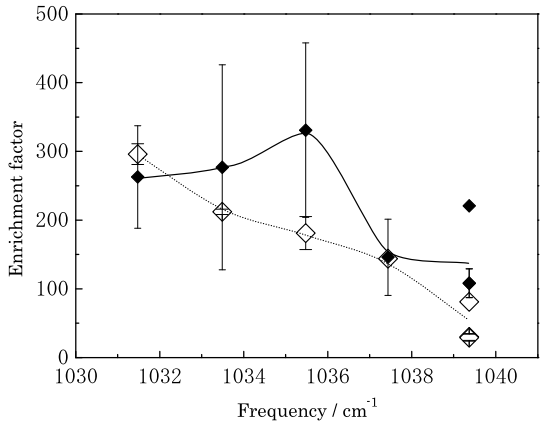

Fig. 3 Dependence of the enrichment factor on dissociation laser frequency at the excitation laser frequency of 1052.2 cm^{-1} (♦) and 1055.7 cm^{-1}(◇). Sample pressure is fixed at 267 Pa. The excitation and dissociation laser fluence are fixed at 0.45 and 1.06 J/cm^2, respectively

3.3 Effect of two-frequency irradiation on dissociation probability

In Table 1, the results of the ^{18}O isotope separation by the two-frequency IRMPD along with the results of the single-frequency IRMPD are summarized. The two-frequency IRMPD reduces the required laser fluence while maintaining the comparable dissociation probabilities and isotope enrichment factors to the single-frequency IRMPD. The total laser fluence is also lower than the fluence in the case

Table 1 Experimental conditions and results for ^{18}O separation. The production rate of ^{18}O is the normalized index for the total number of $C_5H_8{}^{18}O$ molecules which decompose into 2-propenal and ethylene by one laser shot. The excitation laser fluence and dissociation laser fluence are shown as Φ_e and Φ_d, respectively

Laser	Fluence (J/cm^2)		p (kPa)	Irradiation volume (cm^3)	D(^{18}O) (%)	Production rate of $^{18}O^*$	Enrichment factor S
Single frequency	2.1		0.53	0.77	0.043	0.4	751
	2.2		0.27		0.22	1.0	391
	2.6		0.27		1.4	6.4	169
Two frequency	Φ_e	Φ_d					
		1.06	0.53	4.5	0.057	3.0	285
	0.45	1.06	0.27		0.16	4.1	316
		1.22	0.27		0.47	12.5	198

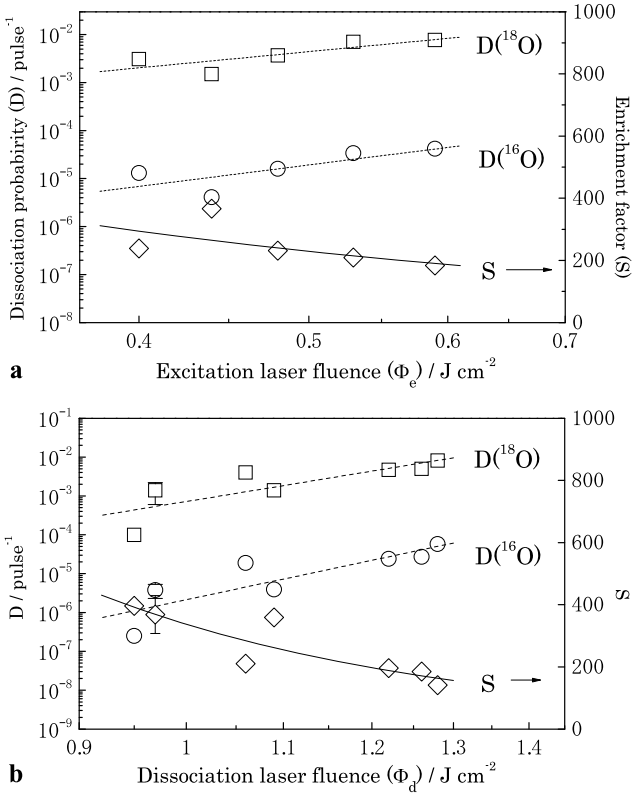

Fig. 4 Dependence of the dissociation probabilities of $C_5H_8{}^{18}O$ (□) and $C_5H_8{}^{16}O$ (○), and enrichment factor (◇) on (**a**) excitation laser fluence and (**b**) dissociation laser fluence. The excitation and dissociation laser frequency are fixed at 1052.2 cm^{-1} and 1031.5 cm^{-1}, respectively. The dissociation laser fluence is fixed at $\Phi_d = 1.13$ J/cm^2 in (**a**) and the excitation laser fluence is fixed at $\Phi_e = 0.45$ J/cm^2 in (**b**). Sample pressure is fixed at 267 Pa

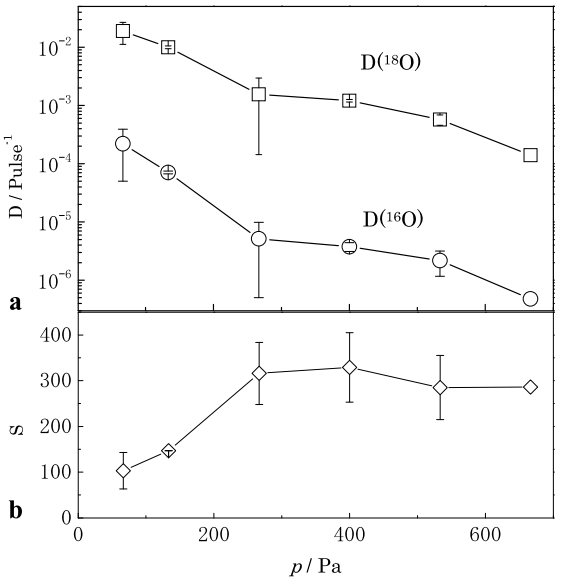

Fig. 5 Dependence of (**a**) dissociation probabilities of (□) $C_5H_8{}^{18}O$ and (○) $C_5H_8{}^{16}O$, and (**b**) enrichment factor on the DHP pressure. The excitation and dissociation laser frequency are fixed at 1052.2 and 1031.5 cm^{-1}, respectively. The excitation and dissociation laser fluence are fixed at 0.45 and 1.13 J/cm^2, respectively

of the single-frequency IRMPD. Since the ^{18}O isotope separation was done under the parallel laser beam condition, the volume of irradiated area was enlarged to five times or more than the volume in the case of the single-frequency IRMPD. Therefore, the production rate of ^{18}O, which is defined as the total number of $C_5H_8{}^{18}O$ dissociated by one laser shot, is remarkably improved. This makes producing a large amount of the enriched C_3H_4O possible.

4 Conclusions

Laser oxygen isotope separation has been done utilizing the isotopically selective IRMPD of DHP under the two-frequency irradiation condition. The laser fluence required to give the same D(^{18}O) as that obtained under the single-frequency irradiation condition was reduced below the damage threshold of the NaCl windows by using the two-frequency irradiation scheme, which is the selective excitation of $C_5H_8{}^{18}O$ molecules to the quasi-continuum state by the excitation laser at low fluence, followed by the further excitation and dissociation of the molecules in the quasi-continuum states by the irradiation of the dissociation laser with lower frequency at relatively high fluence. Since the reduction of required fluence enlarges the irradiation volume, the production rate of ^{18}O can be remarkably improved by using the two-frequency irradiation scheme. The D(^{18}O) and D(^{16}O) increased when the excitation laser frequency is around 1050 cm^{-1}. This enhancement is due to the small absorption peak attributed to the C=C stretching mode.

The pressure dependence of the dissociation probabilities shows that the enrichment factor of ^{18}O increases with increasing pressure and saturates at 267 Pa or higher pressure region. Since D(^{18}O) decreases monotonically with increasing pressure, the pressure should be below 267 Pa to establish both the high enrichment factor and high dissociation probability of $C_5H_8{}^{18}O$.

Acknowledgements This work was partly supported by Research for Promoting Technological Seeds form Japan Science and Technology Agency and by Grant-in-Aid for Scientific Research (B) from the Ministry of Education, Culture, Sports, Science and Technology in Japan (No. 20360422).

References

1. G. Zakrzewska-Tranadel, A.G. Chimelewski, N.R. Miljevic, J. Membr. Sci. **113**, 337 (1996)
2. G. Boato, G. Scoles, M.E. Vallauri, IL Nuovo Cimento, **XIV**(4) (1959)
3. A.M. Rozen, *Teoria Razdelenia Izotopov v Kolonah* (Atomizdat, Moscva, 1960)

4. F. Pop, I. Piciorea, M. Iliescu, M. Culcer, C. Croitoru, I. Stefanescu, Annals of University of Craiova, Electrical Engineering Series (30) (2006)
5. L.A. Webster, N.H. Wahl, H.C. Urey, J. Chem. Phys. **3**, 129 (1935)
6. S. Terabe, T. Yashima, N. Tanaka, M. Araki, Anal. Chem. **60**, 1673 (1988)
7. N. Tanaka, M. Araki, J. Am. Chem. Soc. **107**, 7780 (1985)
8. N. Tanaka, K. Hosoya, K. Nomura, T. Yoshimura, T. Ohki, R. Yamaoka, K. Kimura, M. Araki, Nature **341**, 727 (1989)
9. H.S. Spacil, C.S. Tedman, Nature **222**, 662 (1969)
10. R.C. Bergman, G.F. Homicz, J.W. Rick, G.L. Wolk, J. Chem. Phys. **78**, 1281 (1983)
11. S. Mori, H. Akatsuka, M. Suzuki, J. Nucl. Sci. Technol. **38**, 850 (2001)
12. V.V. Vizhin, Yu.N. Molin, A.K. Petrov, A.R. Sorokin, Appl. Phys. **17**, 385 (1978)
13. T. Majima, K. Sugita, S. Arai, Chem. Phys. Lett. **163**, 29 (1989)
14. V.B. Laptev, E.A. Ryabov, L.M. Tumanova, Quantum Electron. **22**, 607 (1995)
15. D. Garcia, P.M. Keehn, J. Am. Chem. Soc. **100**, 6111 (1978)
16. A. Yokoyama, K. Katsumata, H. Ohba, H. Akagi, M. Saeki, K. Yokoyama, J. Phys. Chem. A **112**, 6571 (2008)
17. A. Yokoyama, H. Ohba, M. Hashimoto, K. Katsumata, H. Akagi, T. Ishii, A. Ohya, S. Arai, Appl. Phys. B **79**, 883 (2004)
18. H. Ohba, H. Akagi, K. Katsumata, M. Hashimoto, A. Yokoyama, Jpn. J. Appl. Phys. **47**, 8379 (2008)
19. M.J. Frisch, G.W. Trucks, H.B. Schlegel, G.E. Scuseria, M.A. Robb, J.R. Cheeseman, J.A. Montgomery Jr., T. Vreven, K.N. Kudin, J.C. Burant, J.M. Millam, S.S. Iyengar, J. Tomasi, V. Barone, B. Mennucci, M. Cossi, G. Scalmani, N. Rega, G.A. Petersson, H. Nakatsuji, M. Hada, M. Ehara, K. Toyota, R. Fukuda, J. Hasegawa, M. Ishida, T. Nakajima, Y. Honda, O. Kitao, H. Nakai, M. Klene, X. Li, J.E. Knox, H.P. Hratchian, J.B. Cross, V. Bakken, C. Adamo, J. Jaramillo, R. Gomperts, R.E. Stratmann, O. Yazyev, A.J. Austin, R. Cammi, C. Pomelli, J.W. Ochterski, P.Y. Ayala, K. Morokuma, G.A. Voth, P. Salvador, J.J. Dannenberg, V.G. Zakrzewski, S. Dapprich, A.D. Daniels, M.C. Strain, O. Farkas, D.K. Malick, A.D. Rabuck, K. Raghavachari, J.B. Foresman, J.V. Ortiz, Q. Cui, A.G. Baboul, S. Clifford, J. Cioslowski, B.B. Stefanov, G. Liu, A. Liashenko, P. Piskorz, I. Komaromi, R.L. Martin, D.J. Fox, T. Keith, M.A. Al-Laham, C.Y. Peng, A. Nanayakkara, M. Challacombe, P.M.W. Gill, B. Johnson, W. Chen, M.W. Wong, C. Gonzalez, J.A. Pople (Gaussian, Inc., Wallingford, 2004)
20. V.N. Bagratashvili, V.S. Letokhov, A.A. Makarov, E.A. Ryabov, Laser Chem. **4**, 171 (1983)